

# $^{10}\text{He}$ low-lying states structure uncovered by correlations

S.I. Sidorchuk,<sup>1</sup> A.A. Bezbakh,<sup>1</sup> V. Chudoba,<sup>1,2</sup> I.A. Egorova,<sup>3</sup> A.S. Fomichev,<sup>1</sup> M.S. Golovkov,<sup>1</sup> A.V. Gorshkov,<sup>1</sup> V.A. Gorshkov,<sup>1</sup> L.V. Grigorenko,<sup>1,4,5</sup> G. Kaminski,<sup>1,6</sup> S.A. Krupko,<sup>1</sup> E.A. Kuzmin,<sup>5</sup> E.Yu. Nikolskii,<sup>5,7</sup> Yu.Ts. Oganessian,<sup>1</sup> Yu.L. Parfenova,<sup>1,8</sup> P.G. Sharov,<sup>1</sup> R.S. Slepnev,<sup>1</sup> S.V. Stepanov,<sup>1</sup> G.M. Ter-Akopian,<sup>1</sup> R. Wolski,<sup>1,6</sup> A.A. Yukhimchuk,<sup>9</sup> S.V. Filchagin,<sup>9</sup> A.A. Kirdyashkin,<sup>9</sup> I.P. Maksimkin,<sup>9</sup> and O.P. Vikhlyantsev<sup>9</sup>

<sup>1</sup>Flerov Laboratory of Nuclear Reactions, JINR, Dubna, RU-141980 Russia

<sup>2</sup>Institute of Physics, Silesian University in Opava, Bezručovo nám. 13, 74601 Czech Republic

<sup>3</sup>Bogolyubov Laboratory of Theoretical Physics, JINR, Dubna, 141980 Russia

<sup>4</sup>GSI Helmholtzzentrum für Schwerionenforschung, Planckstraße 1, D-64291 Darmstadt, Germany

<sup>5</sup>National Research Centre “Kurchatov Institute”, Kurchatov sq. 1, RU-123182 Moscow, Russia

<sup>6</sup>Institute of Nuclear Physics PAN, Radzikowskiego 152, PL-31342 Kraków, Poland

<sup>7</sup>RIKEN Nishina Center, Hirosawa 2-1, Wako, Saitama 351-0198, Japan

<sup>8</sup>Skobeltsyn Institute of Nuclear Physics, Moscow State University, 119991 Moscow, Russia

<sup>9</sup>All-Russian Research Institute of Experimental Physics, RU-607190 Sarov, Russia

(Dated: October 14, 2018. File: `he10-10.tex`)

The  $0^+$  ground state of the  $^{10}\text{He}$  nucleus produced in the  $^3\text{H}(^8\text{He},p)^{10}\text{He}$  reaction was found at about  $2.1 \pm 0.2$  MeV ( $\Gamma \sim 2$  MeV) above the three-body  $^8\text{He}+n+n$  breakup threshold. Angular correlations observed for  $^{10}\text{He}$  decay products show prominent interference patterns allowing to draw conclusions about the structure of low-energy excited states. We interpret the observed correlations as a coherent superposition of the broad  $1^-$  state having a maximum at energy 4–6 MeV and the  $2^+$  state above 6 MeV, setting both on top of the  $0^+$  state “tail”. This anomalous level ordering indicates that the breakdown of the  $N = 8$  shell known in  $^{12}\text{Be}$  thus extends also to the  $^{10}\text{He}$  system.

PACS numbers: 24.50.+g, 24.70.+s, 25.45.Hi, 27.20.+n

*Introduction.* With the improvement of knowledge about the nuclei far from the “stability valley” and with the development of experimental techniques the interests of researchers are naturally shifting to the regions beyond the nuclear stability lines. The understanding of such systems is indispensable for deeper insights into the nuclear dynamics, for further development of nuclear models, and for nuclear astrophysics applications. Among the isotopes observed as resonances  $^{10}\text{He}$  has the largest  $N/Z$  ratio on nuclear chart, thus representing the most extreme nuclear matter asymmetry. According to natural shell-model considerations  $^{10}\text{He}$  should be the second lightest double-magic nucleus after  $^4\text{He}$ . However, the search for nuclear-stable  $^{10}\text{He}$  was in vain and in 1994 it was observed as a resonance [1]. Thus an additional stabilizing effect of shell closure was not observed. Our new results cast even more doubt in magic nature of this nucleus giving less binding than expected [1–3] and providing evidence for the low-lying negative parity intruder state.

This isotope is difficult to study as there are very few ways to produce the nucleus with such an enormous neutron excess. There are several qualitatively different experimental results on the  $^{10}\text{He}$  spectrum. A *broad* ( $\Gamma \lesssim 1.2$  MeV) resonance at energy  $E_T = 1.2(3)$  MeV was observed [1] as a result of proton knockout from  $^{11}\text{Li}$  ( $E_T$  is the energy relative to the three-body  $^8\text{He}+n+n$  decay threshold). A very similar excitation spectrum was obtained for  $^{10}\text{He}$  in the analogous reaction at higher beam energy [2]. However, the authors of this work came to somewhat different parameters for the  $0^+$   $^{10}\text{He}$  ground state (g.s.) resonance:  $E_T = 1.5$  MeV

and  $\Gamma = 1.9$  MeV. Also the existence of  $2^+$  excited state was inferred with  $E_T = 4$  MeV and  $\Gamma = 1.6$  MeV basing on three-body  $^8\text{He}+n+n$  correlations [3]. The authors of Ref. [4] reported a *narrow* ( $\Gamma = 0.3$  MeV)  $^{10}\text{He}$   $0^+$  g.s. at  $E_T = 1.07(7)$  MeV populated in a double charge-exchange reaction. Besides, the two peaks at 4.3 and 7.9 MeV [4] were interpreted as excited states of  $^{10}\text{He}$  with spin-parities  $2^+$  and  $3^-$ .

Neutron transfer is known to be a reliable tool for the study of nuclear systems with large neutron excess. No  $^{10}\text{He}$  resonance peak in the vicinity of  $E_T \sim 1$  MeV was found in the  $2n$  transfer reaction  $^3\text{H}(^8\text{He},p)^{10}\text{He}$  [5]. The observed  $^{10}\text{He}$  spectrum showed a *broad* group of events at 2.5–4.5 MeV. In this Letter we report about a refined experiment on the  $^3\text{H}(^8\text{He},p)^{10}\text{He}$  reaction which gives the  $^{10}\text{He}$  g.s. position at  $E_T \sim 2.1$  MeV. The new work comprises a convincing statistics with correlation results enabling spin-parity assignments.

*Experiment.* A primary  $^{11}\text{B}$  beam with energy 36A MeV was delivered by the U-400M cyclotron (JINR, Dubna). The secondary 21.5A MeV beam of  $^8\text{He}$  with intensity  $\sim 1.5 \cdot 10^4$   $s^{-1}$  obtained with the fragment-separator ACCULINNA [6] hit a gaseous tritium target [7], see Fig. 1. The two thin plastic scintillators set on a 8 m base before the target allowed the beam particle identification and the time-of-flight (TOF) measurement with an accuracy of about 0.5 ns. The two multiwire proportional chambers performed tracking for incoming  $^8\text{He}$  ions providing hit positions on the target cell with accuracy  $\sim 1.5$  mm. The target windows of 25 mm in diameter were sealed with two pairs of 8.4  $\mu$  stainless steel foils. The 6 mm thick target cell was filled with tritium with a

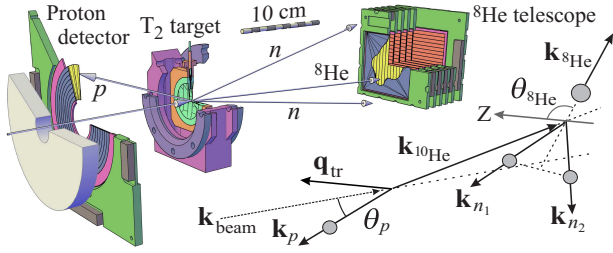


FIG. 1. Experimental layout and kinematical scheme for the  $^3\text{H}(^8\text{He},p)^{10}\text{He}$  reaction. The proton and  $^{10}\text{He}$  momenta are shown in the lab system, the variables applied to the  $^{10}\text{He}$  decay products are presented in the  $^{10}\text{He}$  center-of-mass system with Z axis parallel to the transferred momentum vector.

gas pressure of 0.92 atm and cooled down to 26 K. The total integral flux of  $^8\text{He}$  was  $\sim 1.4 \cdot 10^{10}$ . The concept of the experiment was similar to that applied in our previous works [8–10]. This approach implies the detection of recoil protons emitted from the target in backward direction in the lab system. This low-background kinematical range corresponds to small angles in the center-of-mass (c.m.) system. The protons were detected with a 1 mm thick annular Si detector with the inner and outer diameters of its sensitive area of 32 and 82 mm, respectively. The two detector sides were segmented in 16 rings and 16 sectors. With the proton detector installed 100 mm upstream the target the  $^{10}\text{He}$  missing mass was measured with resolution of about 0.5 MeV (FWHM). This estimate followed from a Monte-Carlo simulation and was found to be in a good agreement with the results obtained for the  $^3\text{H}(^6\text{He},p)^8\text{He}$  reaction populating the well known  $0^+$  and  $2^+$  states of  $^8\text{He}$ . A telescope composed of six square, 1 mm thick,  $61 \times 61 \text{ mm}^2$  Si detectors (having 16 strips each) was placed 250 mm downstream the target to detect the  $^8\text{He}$  fragments originating from the  $^{10}\text{He}$  decay in coincidence with the recoil protons.

*“Triangle” presentation of the data.* The energy  $E(^8\text{He})$  of  $^8\text{He}$  in the c.m. of  $^{10}\text{He}$  is plotted vs.  $E_T$  in Fig. 2 (a). This presentation allows to estimate background conditions and reject events located outside the kinematically allowed region. Events appearing below the solid line in Fig. 2 (a) satisfy the condition  $E(^8\text{He}) < E_T/5$ . To take into account the experimental resolution we present below results obtained for events located inside the broader shaded triangle. The background inside the triangle was measured in irradiations made with empty target and was found to be negligible.

*Missing mass of  $^{10}\text{He}$ .* The projected missing mass spectrum from the data of Fig. 2 (a) is shown by points with error bars in Fig. 2 (b). The  $^{10}\text{He}$  g.s. peak is clearly seen at about 2.1 MeV. Above the g.s. the spectrum is quite featureless showing a smooth rise after 4 MeV. Superimposed on the experimental points in Fig. 2 (b) is the  $J^\pi = 0^+$  g.s. spectrum of  $^{10}\text{He}$  theoretically predicted in Ref. [11]. Note the good correspondence between experimentally observed spectrum and theory within the main

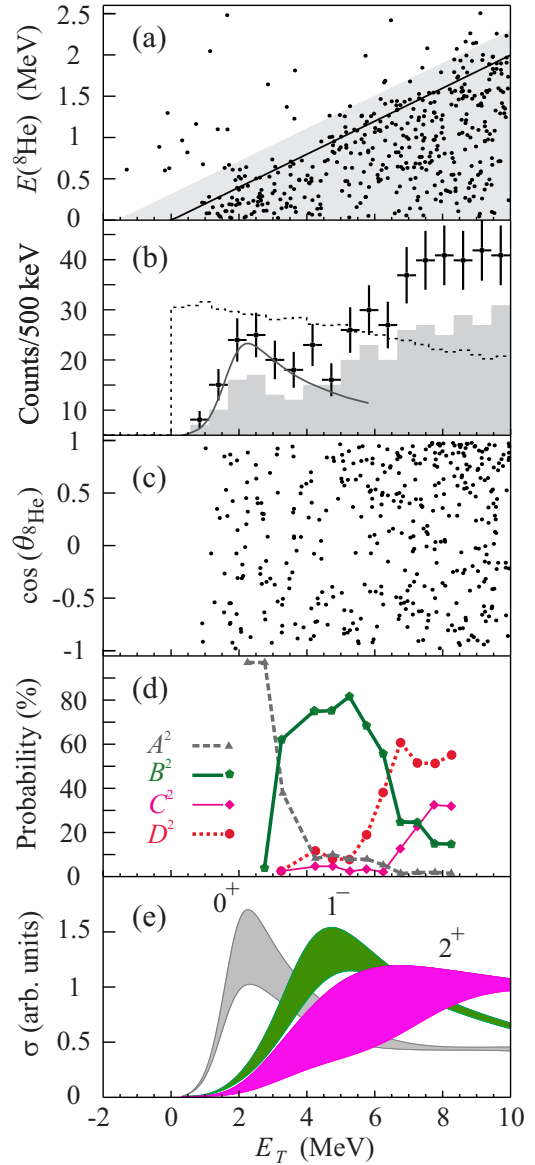


FIG. 2. (a) Scatter plot of  $E(^8\text{He})$  vs.  $E_T$ . (b)  $^{10}\text{He}$  missing mass spectrum. Points with error bars correspond to the total bulk of events, while the grey histogram is obtained under condition  $\varepsilon < 0.5$ . The dotted histogram shows the detection efficiency. The theoretical curve from the panel (e) is given to guide eye. (c) Angular distribution of  $^8\text{He}$  in the  $^{10}\text{He}$  c.m. frame. (d) Squared amplitudes (they do not change signs) of different partial contributions in Eq. (1) deduced from the angular distribution. (e) Theoretically predicted  $^{10}\text{He}$  spectra for different  $J^\pi$ . Shaded areas reflect the uncertainty of these calculations.

part of the  $^{10}\text{He}$  g.s. peak.

*Angular distribution of  $^8\text{He}$ .* Angular correlations obtained for  $^8\text{He}$  emitted from  $^{10}\text{He}$  were analyzed using a specific frame with Z axis coinciding in the direction with the transferred momentum vector  $\mathbf{q}_{\text{tr}} = (1/4)\mathbf{k}_{\text{beam}} - \mathbf{k}_p$ . The angular distribution of  $^8\text{He}$  vs.  $^{10}\text{He}$  decay energy is shown in Fig. 2 (c). Three regions with prominent

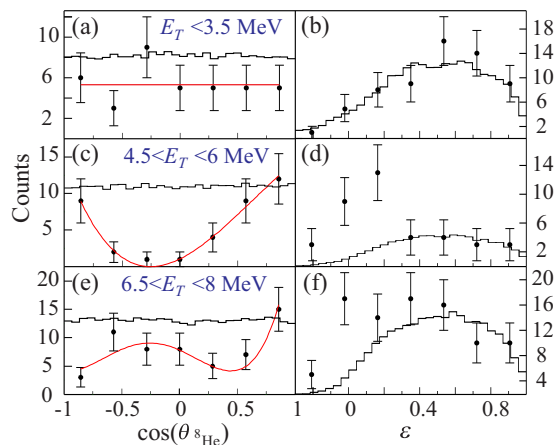


FIG. 3. Panels (a,c,e) show the angular distributions of  ${}^8\text{He}$  measured in different energy ranges of  ${}^{10}\text{He}$  excitation. Curves show fits made by using Eq. (1). Panels (b,d,f) present energy distributions between neutrons obtained for the same energy ranges. Dots with error bars are experimental data, the histograms show the detection system response to the phase volume.

and qualitatively different correlation patterns are seen in this plot: (i) “ $s$ -wave” range  $E_T < 4$  MeV, (ii) “ $s/p$  interference” range  $4 < E_T < 6$  MeV, (iii) “ $s/p/d$  interference” range  $6 < E_T < 8$  MeV. The angular distributions for these energy ranges obtained under the condition  $\varepsilon = E_{nn}/E_T < 0.5$  ( $E_{nn}$  is the  $n-n$  relative energy) are shown in Fig. 3 (a,c,e) together with fits obtained by the expression

$$w = \left[ AP_0(x) + B\sqrt{3}P_1(x) + C\sqrt{5}P_2(x) \right]^2 + D^2. \quad (1)$$

Here  $P_l$  are Legendre polynomials with  $x = \cos(\theta_{s\text{He}})$ . Coefficients  $A$ ,  $B$  and  $C$  are the amplitudes of coherent  $s$ -,  $p$ - and  $d$ -wave contributions, respectively, while  $D$  takes into account a decoherent “background”. The energy behavior of these amplitudes is presented in Fig. 2 (d). We put an additional condition  $\varepsilon < 0.5$  as in the limiting case  $\varepsilon \rightarrow 1$  the angle  $\theta_{s\text{He}}$  becomes degenerate. It is also obvious that at  $\varepsilon$  close to unity this angle is poorly defined from data due to errors in the momentum reconstruction.

Note the region (ii) [Fig. 3 (c)] where the distribution tends to zero around small  $|\cos(\theta_{s\text{He}})|$  indicating that only *coherent contributions* take place in this energy range. Why there are such expressed correlation patterns for  ${}^8\text{He}$  fragment distribution and how they could be connected to the quantum numbers of the whole  ${}^{10}\text{He}$  system? In our analysis we base on earlier experience obtained in analogous correlation studies of the three-body decay of the  ${}^5\text{H}$  system ( $t+n+n$  channel) populated in the ( $t,p$ ) transfer reaction [8, 9]. In such three-body systems prominent correlation patterns could be formed if the reaction mechanism is one-step (a direct reaction mechanism) and the transferred spin is zero ( $\Delta S = 0$ ).

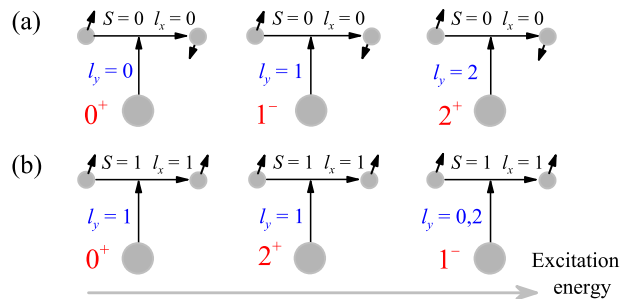


FIG. 4. Expected major components of  ${}^{10}\text{He}$  wave function with different  $J^\pi$  in the cluster  ${}^8\text{He}+n+n$  representation. The rows (a) and (b) demonstrate the two sets of components which may interfere in the angular distributions of  ${}^8\text{He}$  in the  ${}^{10}\text{He}$  c.m. frame. States with different  $J^\pi$  are ordered by energy position expected for a particular configuration.

For such conditions the formed correlations could be revealed in the frame where  $Z$  axis coincides with the transferred momentum vector, because only zero magnetic substates of orbital momentum are transferred resulting in the population of completely aligned configurations in the final state.

To understand how the alignment of the whole three-body system is converted into the expressed correlation patterns for the selected  ${}^8\text{He}$  fragment one needs to consider the structure of the  ${}^{10}\text{He}$  states. There are two sets of possible major configurations for the  ${}^{10}\text{He}$  wave function with different  $J^\pi$  which interfere with each other, see Fig. 4. The set with  $S = 1$  can be rejected for the following reasons: (i) the transfer of two neutrons with  $S = 1$  configuration is very unlikely. Extensive experience gained in ( $t,p$ ) reaction studies points to strong dominance of “dineutron” ( $S = 0$  “particle”) transfer; (ii)  ${}^8\text{He}$  in  $p$ -wave configuration ( $l_y = 1$ ) for the g.s. leads to a contradiction, compare Fig. 3 (a) and Fig. 4 (b); (iii) for the  $0^+$  and  $2^+$  states the orbital momentum  $l_y$  of  ${}^8\text{He}$  is coupled with the orbital momentum  $l_x$  of two neutrons to total orbital momentum  $L = 1$ . Complete alignment of  $L$  does not mean any specific alignment of the  ${}^8\text{He}$  orbital momentum  $l_y$ . In contrast, for the  $S = 0$  configurations the  $l_x = 0$  dominance is expected and complete alignment of the total orbital momentum  $L$  is immediately transferred into a complete alignment of  ${}^8\text{He}$  orbital momentum  $l_y$ . In this case the amplitudes for the angular distributions of  ${}^8\text{He}$  in the selected  ${}^{10}\text{He}$  c.m. frame are obtained as a result of coherent summation of Legendre polynomials  $P_l^0(x)$ . This provides the explanation for Eq. (1).

Level ordering  $0^+$ ,  $1^-$ ,  $2^+$  is inferred from the configuration choice shown in Fig. 4 (a). Thus, the correlation data provide evidence for anomalous level ordering in  ${}^{10}\text{He}$ . For the  $1^-$  state the proposed correlation analysis gives the energy and width around 5.5 and 2.5 MeV, respectively. For the  $2^+$  state we can establish only an energy range where the corresponding set of quantum numbers is important, see Fig. 2 (d).

The interpretation of the data presented in this section is *minimal required*. Indeed, the Legendre polynomials with  $l$  not less than 1 are needed to describe the angular distribution in the energy range  $4 < E_T < 6$  MeV. Then, a visible asymmetry of the angular distribution presented in Fig. 3 (c) is a proof for the positive/negative parity state interference. Taking into account the structural arguments of Fig. 4 we conclude that the  $s/p$  interference is a *minimal required* set of components for this energy range. Analogous argumentation leads to the  $s/p/d$  assignment for the energy range  $6 < E_T < 8$  MeV, see Fig. 3 (e). More complex interpretations would require much more conditions to be fulfilled strictly and simultaneously.

*Energy distributions in  $^{10}\text{He}$ .* Additional qualitative support for the conclusion made about the population of different states at  $E_T < 4$  MeV,  $4 < E_T < 6$  MeV, and  $6 < E_T < 8$  MeV can be found in the energy correlations occurring within these ranges, see Fig. 3 (b,d,f). The energy distribution parameter  $\varepsilon$  shows how the energy is shared between the  $^8\text{He}$  and “dineutron” subsystems. This distribution is close to the phase volume for the ground state, see Fig. 3 (b). However, it is qualitatively different for the excited states where the “dineutron” energy correlations ( $\varepsilon \sim 0$ ) are enhanced. This effect is especially strong for the energy range  $4 < E_T < 6$  MeV where the  $1^-$  state shows up. The observation of the expressed “dineutron” energy correlations is an additional argument supporting the  $\Delta S = 0$  transfer in our experiment, see discussion of Fig. 4 above. We can expect the low-energy enhancement in the  $n$ - $n$  channel in the case of attractive  $n$ - $n$  final state interaction available in the  $S = 0$ ,  $l_x = 0$  configurations.

*Theoretical calculations.* The g.s. of  $^{10}\text{He}$  was extensively studied theoretically in Ref. [11] focusing on a possible existence of a “three-body virtual state” (an extremely low-energy peak with  $[s_{1/2}^2]$  structure). Several versions of calculations were provided depending on the scattering length in the  $^8\text{He}$ - $n$  channel. The recent experimental results [2, 10] do not support the existence of a virtual state in  $^9\text{He}$  with a large negative scattering length. So, considering the  $^{10}\text{He}$  g.s. we can stick to the predictions based on the  $^8\text{He}$ - $n$  interactions with the  $s$ -wave scattering length around zero. Such calculations provide the g.s. of  $^{10}\text{He}$  with the dominant  $[p_{1/2}^2]$  structure at about 2 MeV in a nice agreement with the present experimental result, see Fig. 2 (e).

According to calculations [11] the results reported in Refs. [1, 2] do not contradict the g.s. energy of  $^{10}\text{He}$  obtained in the present work. In these works the  $^{10}\text{He}$  spectrum was populated by the proton knockout from  $^{11}\text{Li}$ . It was demonstrated in [11] that the  $^{10}\text{He}$  g.s. observed at about 2.0 – 2.5 MeV in “conventional” reactions [like the  $(t,p)$  transfer used in our work] should have observable position 1.0 – 1.5 MeV for the reactions with  $^{11}\text{Li}$  due to the strong initial state effect. The observable g.s. peak position is shifted towards lower energy because of the abnormal size of  $^{11}\text{Li}$  possessing one of the most de-

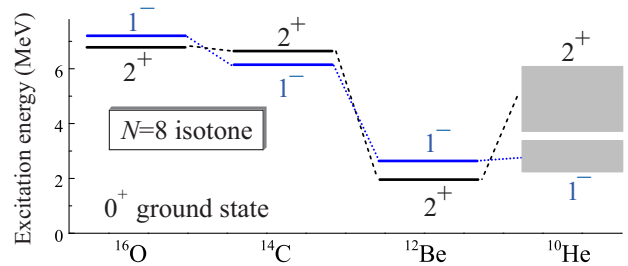


FIG. 5. Low-lying  $2^+$  and  $1^-$  states for the  $N = 8$  isotone chain of  $p$ -shell nuclei. Gray rectangles indicate the uncertainty of the  $^{10}\text{He}$  level positions in our analysis.

veloped known neutron halos.

In this Letter we extend the calculations of Ref. [11] to the  $1^-$  and  $2^+$  excitations of  $^{10}\text{He}$ . The model predictions for the  $^{10}\text{He}$  spectrum population give quite broad structures with very asymmetric shapes, see Fig. 2 (e). The shaded areas show the ranges provided by theoretical calculations with a realistic parameter variation. The calculation results are very stable for the g.s. energy but demonstrate increasing uncertainty for the higher-lying excitation spectra. However, in all the calculations the lowest excitation is  $1^-$  providing additional support to the proposed experimental spin assignment.

*Discussion.* Observation of the  $1^-$  configuration as the first excited state in  $^{10}\text{He}$  is the most intriguing finding of this work. The existence of such low-lying excitations is not something totally unexpected in the nearby exotic nuclei. Such excitations in the form of *soft dipole mode* are known for  $^6\text{He}$  [12],  $^{11}\text{Li}$  [13] and there is evidence that  $1^-$  is the lowest excitation of  $^8\text{He}$  [5].

The importance of the intruder configuration is evident in  $^{11}\text{Be}$  where the existence of neutron halo is connected to the anomalous  $1/2^+$  spin-parity of the ground state. In the  $^{12}\text{Be}$  spectrum the breakdown of the  $N = 8$  shell closure is seen due to the existence of the low-lying  $1^-$  state. The importance of this phenomenon was broadly discussed both from experimental [14, 15] and theoretical points of view [16, 17]. Our results provide novel information on the evolution of low-lying level ordering of the  $N = 8$  isotones, see Fig. 5. In  $^{10}\text{He}$  the  $1^-$  state is found to be at the energy comparable to that in  $^{12}\text{Be}$ , while the  $2^+$  state is at the energy comparable to that in the other members of the isotone chain.

*Conclusions.* The low-lying spectrum of  $^{10}\text{He}$  was studied in the transfer reaction  $^3\text{H}(^8\text{He},p)^{10}\text{He}$ . The  $0^+$  g.s. energy and width are found to be  $2.1 \pm 0.2$  and  $\sim 2$  MeV, respectively. Owing to specific angular correlations for the first time the spin-parity assignment is made for the low-lying states of  $^{10}\text{He}$ : the analysis of experimental data allowed to interpret the  $^{10}\text{He}$  spectrum as a superposition of the  $0^+$ ,  $1^-$  ( $E_T > 4$  MeV) and  $2^+$  ( $E_T > 6$  MeV) states. The established level sequence shows that  $^{10}\text{He}$  is one more dripline nucleus demonstrating the shell structure breakdown.

*Acknowledgments.* The authors are grateful to Profs.

B. Jonson, M.V. Zhukov, S.N. Ershov and I.G. Mukha for useful discussions. This work was supported by the Russian RFBR 11-02-00657-a grant. L.V.G., S.A.K., A.V.G., and I.A.E. are supported by FAIR-Russia Research Cen-

ter grant. L.V.G. acknowledges the support by HIC for FAIR research grant, and Russian Ministry of Industry and Science grant NSh-7235.2010.2.

- 
- [1] A.A. Korshennikov *et al.*, Phys. Lett. **B326**, 31 (1994).
  - [2] H.T. Johansson *et al.*, Nucl. Phys. **A842**, 15 (2010).
  - [3] H.T. Johansson *et al.*, Nucl. Phys. **A847**, 66 (2010).
  - [4] A.N. Ostrowski *et al.*, Phys. Lett. **B338**, 13 (1994).
  - [5] M.S. Golovkov *et al.*, Phys. Lett. **B672**, 22 (2009).
  - [6] A.M. Rodin *et al.*, Nucl. Phys. **A626**, 567c (1997).
  - [7] A.A. Yukhimchuk *et al.*, Nucl. Instr. Meth. **A513**, 439 (2003).
  - [8] M.S. Golovkov *et al.*, Phys. Rev. Lett. **93**, 262501 (2004).
  - [9] M.S. Golovkov *et al.*, Phys. Rev. C **72**, 064612 (2005).
  - [10] M.S. Golovkov *et al.*, Phys. Rev. C **76**, 021605(R) (2007).
  - [11] L.V. Grigorenko and M.V. Zhukov, Phys. Rev. C **77**, 034611 (2008).
  - [12] T. Aumann, Eur. Phys. J. A **26** (2005) 441.
  - [13] T. Nakamura *et al.*, Phys. Rev. Lett. **96**, 252502 (2006).
  - [14] H. Iwasaki *et al.*, Phys. Lett. **B491**, 8 (2000).
  - [15] S.D. Pain *et al.*, Phys. Rev. Lett. **96**, 032502 (2006).
  - [16] B.A. Brown, Prog. Part. Nucl. Phys. **47**, 517 (2001).
  - [17] G. Gori, F. Barranco, E. Vigezzi and R.A. Broglia, Phys. Rev. C **69**, 041302(R) (2004).